

DRAFT  
UPR/216E  
Princeton/HEP/92-07  
SSCL/PP/139  
August 13, 1992

# Monte Carlo Simulations of $B_d^0 \rightarrow \pi^+\pi^-$ from $p$ - $p$ Interactions at $\sqrt{s} = 40$ TeV

O. R. Long, N. S. Lockyer, P. T. Keener, and F. Azfar  
*David Rittenhouse Laboratories, University of Pennsylvania,  
Philadelphia, PA 19104-6396*

K.T. McDonald, J. G. Heinrich  
*Joseph Henry Laboratories, Princeton University,  
Princeton, NJ 08544*

L. A. Roberts  
*Superconducting Super Collider Laboratory,  
Dallas, TX 75237*

## Abstract

We have studied the identification of the  $CP$ -violating decay  $B_d^0 \rightarrow \pi^+\pi^-$  in the presence of a large hadronic background using the event-generator ISAJET and detector-simulation-package GEANT. The study was performed using  $\sim 10^6$   $b\bar{b}$  events generated and simulated at SSC collider energies. Backgrounds were studied with bottom-, charm- and light-quark events. We found that the principal background comes from  $b\bar{b}$  events, not charm- or light-quark events. After all cuts, we found an efficiency of 4% for finding the decay mode  $B_d^0 \rightarrow \pi^+\pi^-$  with a signal-to-noise ratio of  $> 0.42$ , 90% confidence level. These results indicate the identification of  $B_d^0 \rightarrow \pi^+\pi^-$  decays will be clean and studies of  $CP$  violation at the SSC, beyond those already anticipated with  $B_d^0 \rightarrow J/\psi K_S^0$ , will be possible.

# 1 Introduction

The  $b\bar{b}$  cross section at the SSC is predicted to be 1-3 mb [1], *i.e.*, 1-3% of the  $p$ - $p$  interactions will produce a  $b\bar{b}$  pair. Based on the experience of the CDF collaboration [3, 4], it has been established that the  $B \rightarrow J/\psi X$  modes, which are useful for studies of  $CP$  violation [2], can be found with acceptable background levels in a hadron collider.

This paper reports studies of the efficiency for reconstructing the decay  $B_d^0 \rightarrow \pi^+\pi^-$  and of rejection of relevant backgrounds [5]. This decay is expected to manifest  $CP$  violation, but depends on a different combination of phases of the C-K-M matrix elements than the decay  $B \rightarrow J/\psi K_S^0$ , while remaining free from ambiguity due to strong phases as the  $\pi^+\pi^-$  is in a  $CP$  eigenstate. Identification of this decay mode is expected to be more difficult than the  $B \rightarrow J/\psi X$  modes due to severe combinatoric backgrounds [6]. Nonetheless, two aspects of  $B$  decays will make it possible to extract the  $B_d^0 \rightarrow \pi^+\pi^-$  signal at a hadron collider. The relatively long lifetime of the  $B$  meson ( $1.3 \times 10^{-12}$  sec) allows the vertex for the decay  $B_d^0 \rightarrow \pi^+\pi^-$  to be easily isolated from the primary vertex. In addition, the pions in this decay have the maximum momentum of daughters from any  $B$  decay and so are more readily separated from low- $P_T$  hadron backgrounds.

The results reported here are based on very detailed simulation of pattern recognition in vertex fitting using information from a silicon vertex detector. However, the separate issue of track pattern recognition is not addressed, and it is assumed that detector hits are all properly associated with tracks. A study that combines the issues of track and vertex pattern recognition has been reported elsewhere [7].

## 2 Detector Parameters

We simulated a vertex detector that consisted of three coaxial silicon barrels and 33 silicon disks normal to the beam, 21 of which were interleaved with the barrels. The vertex detector surrounded a beryllium beam pipe as shown in Figure 1. We present the detector geometry and parameters used in the simulation [8]:

- Beryllium Beam Pipe
  1. 400  $\mu\text{m}$  thick
  2. radius = 1.3 cm
  3. length =  $\pm 110$  cm
- Silicon Disks
  1. 200  $\mu\text{m}$  thick
  2.  $1.5 \text{ cm} < \text{radius} < 13.5 \text{ cm}$
  3. 21 central disks at 4 cm spacing

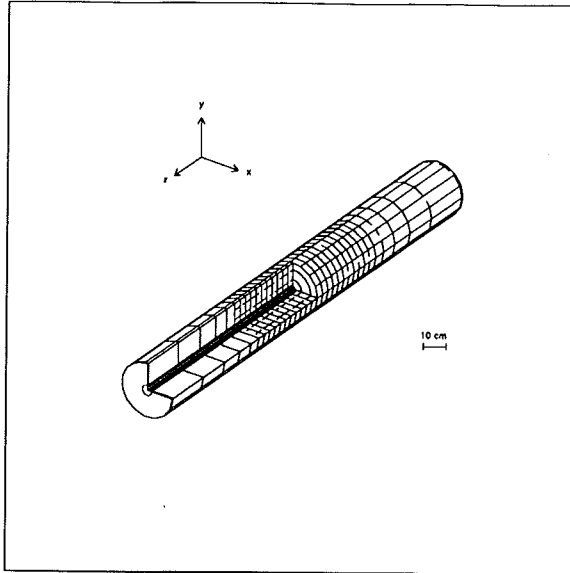


Figure 1: A cut-away view of the simulated detector.

4. 12 pseudorapidity-spaced disks
- Silicon Barrels
  1. 200  $\mu\text{m}$  thick
  2. length = 3.98 cm per segment
  3. 20 inner barrel segments, radius = 1.5 cm
  4. 22 middle barrel segments, radius = 5.0 cm
  5. 22 outer barrel segments, radius = 10.0 cm

### 3 Event Generation

ISAJET [9] was used to generate 1,040,000  $b\bar{b}$  events at 40-TeV center-of-mass energy. In addition, 400,000 charm and 320,000 all-jet events were generated for background studies. GEANT [10] decayed the particles and then tracked them through the detector layers, including effects of multiple scattering (*a la* Molière), nuclear interactions and electromagnetic cascades. The detector simulation contained a beam pipe and silicon vertex detector with no magnetic field.

Roughly 42% of the  $b\bar{b}$  events contained  $B_d^0$  mesons, which were forced to decay to  $\pi^+\pi^-$  to provide a large sample of signal decays. A  $\bar{B}$  meson in these events decayed according to a standard table of branching ratios and decay products [11], to provide a sample of  $\bar{B}$  decays that could be used to estimate the probability of faking a  $\pi^+\pi^-$  decay. Table 1 shows the number of decay modes and average multiplicity of decay products for some of the  $B$  and  $D$  mesons considered in this study.

Table 1: The number of decay modes and average multiplicity of decay products for some of the  $B$  and  $D$  mesons in the GEANT decay table used in this simulation [11].

Particle	Number of Decay Modes	Average Multiplicity
$B_d^0$	145	4.1
$B^+$	196	4.9
$D^0$	78	4.1
$D^+$	57	4.0
$D_s^+$	81	3.6

The simulation was run on Intel iPSC/860 processors at U. Pennsylvania and the SSC Laboratory [12]. We used up to 16 independent processors (nodes) simultaneously generating  $\sim 1,650$  events/hour on each node.

## 4 Vertex Reconstruction

Only charged tracks were used for vertex reconstruction, and these were required to have at least three hits in the disk detectors or three hits in the barrels, where a hit is defined as a track intercepting a silicon detector with angle of incidence less than  $55^\circ$ . To simulate the effect of detector resolution, the hits were spatially smeared with Gaussian errors based on angle-dependent resolution measured for silicon detectors with  $25\text{-}\mu\text{m}$  strips read out every second strip [13]. The resolution was best near  $0^\circ$  angle of incidence (normal incidence) with a value of  $4\text{ }\mu\text{m}$  and increased to  $16\text{ }\mu\text{m}$  at  $55^\circ$  angle of incidence. Disk hits were smeared in  $x$  and  $y$ , where the  $z$  axis is along the beam. A rotation about the  $z$ -axis was used for smearing the barrel hits. The  $x$ -axis was rotated to point towards the innermost barrel hit. The new  $x$ -axis was called the  $u$ -axis and the new  $y$ -axis was called the  $v$ -axis. After the rotation, the barrel hits were smeared in  $z$  and  $v$ .

A straight line was fit to the hits for each track, giving a slope, intercept and error matrix based on the assumed detector resolution and on the r.m.s. estimate of multiple scattering the track had suffered prior to the detection point. (This estimate of multiple scattering depends on a knowledge of the momentum of the charged particle, assumed known from an outer tracking detector not simulated.) Fitted tracks with  $P_T > 0.6\text{ GeV}/c$  and pseudorapidity  $|\eta| < 4$  were then passed to a vertexing algorithm VERTEX (X1023), taken from the CERN Program Library. Low- $P_T$  tracks were excluded from vertexing because they suffer significant multiple scattering and can readily produce false signatures of secondary vertices. The pseudorapidity cut was applied to insure that tracks were not too near the boundary of this simulation

at  $\eta = 5$ .

All remaining tracks were first fit to the hypothesis of a single vertex. Tracks that fit poorly to this hypothesis were passed to the next iteration of the vertexing procedure as candidates for fits to secondary vertices. At each iteration only tracks with vertex  $\chi^2 < 3$  were assigned to the vertex hypothesis of that iteration (after which the vertex parameters were refit using only the good tracks). The vertex from the first set of four or more well-fitting tracks was defined as the reconstructed primary interaction point. The fitting procedure was iterated until no more satisfactory secondary vertices could be found.

It is useful to define a number which represents the amount of background rejection performance required from the vertex detector in order that the  $B_d^0 \rightarrow \pi^+\pi^-$  signal be observed. A vertex rejection factor is defined by the following ratio:

$$\frac{\text{All oppositely charge pairs} \\ \text{with } P_T > 1.75 \text{ GeV}/c \text{ and } |\eta| < 4}{\text{All two-track vertices selected after cuts.}}$$

It was found to be  $\approx 2500$ .

The secondary vertices that contained only two tracks of opposite sign were considered as  $B_d^0 \rightarrow \pi^+\pi^-$  candidates. The associated tracks were converted to 4-vectors for invariant-mass analysis by assuming they were pions and combining the track angles reconstructed in the vertex detector with a momentum ‘reconstructed’ simply by smearing the true momentum with Gaussian errors of  $\sigma_P/P = 0.001P \text{ GeV}/c$  to approximate the resolution of an outer tracking detector.

The vertexing algorithm successfully reconstructed decays of particles other than  $B_d^0$  as Figure 2 shows. The invariant-mass calculation for Figure 2 used the correct masses for the decay products assuming particle identification.

## 5 $B_d^0 \rightarrow \pi^+\pi^-$ Analysis

The candidate  $B_d^0 \rightarrow \pi^+\pi^-$  data sample consisted of all opposite sign, two-track vertices found by the procedure outlined in the previous section. Only 11% of the true  $B_d^0 \rightarrow \pi^+\pi^-$  decays passed the initial  $P_T$ ,  $|\eta|$  and vertex- $\chi^2$  cuts.

Three additional cuts were applied to improve the signal-to-noise for reconstruction of  $B_d^0 \rightarrow \pi^+\pi^-$  decays:

1. The closest-distance-of-approach cut.
2. The vertex-separation cut ( $S/\Delta S$ ).
3. The track- $P_T$  cut.

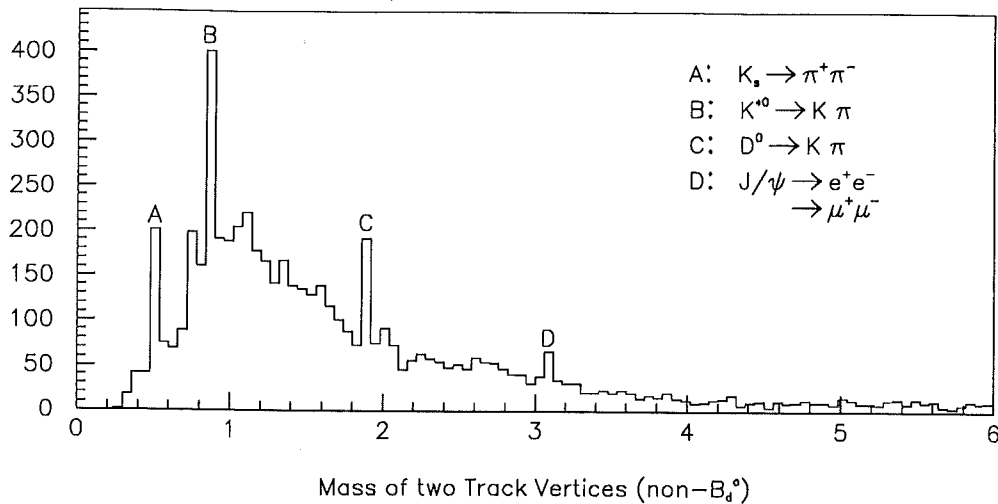


Figure 2: Reconstructed decays from  $p$ - $p$  events at  $\sqrt{s} = 40$  TeV producing  $b\bar{b}$  pairs only.

The closest distance of approach (CDA) between the 3-momentum of candidate  $B$ 's and the reconstructed primary vertex is shown in Figure 3<sup>1</sup>. In the absence of multiple scattering and measurement error the total 3-momentum of the products of a  $B$  decay would point back directly to the primary vertex, while a fake  $B_d^0 \rightarrow \pi^+\pi^-$  decay may well have total 3-momentum that does not emanate from the primary vertex. The upper-left graph of Figure 3 shows the CDA distribution for the so-called  $B^0$  sample in which the tracks actually came from a  $B_d^0 \rightarrow \pi^+\pi^-$  decay, and the upper-right graph shows the distribution for 'non- $B^0$ ' track pairs in which the tracks do not come from a  $B_d^0 \rightarrow \pi^+\pi^-$  decay (but may come from another  $B$  in the event). Events with  $\text{CDA} < 0.01$  cm were retained as  $B_d^0 \rightarrow \pi^+\pi^-$  candidates. The CDA cut kept 95% of the signal and removed 50% of the background.

A parameter that measures the statistical significance of the separation of the primary vertex from the secondary vertex was called  $S/\Delta S$ , where  $S$  was the (reconstructed) distance between the primary vertex and the secondary vertex of the candidate  $B_d^0 \rightarrow \pi^+\pi^-$  decay, and  $\Delta S$  is the error on  $S$  calculated from the error matrices of the two vertices. Many reconstructed secondary vertices are actually due to tracks from the primary vertex with small measurement errors that fit to hypotheses of vertices only slightly separated from the primary. Figure 4 shows the  $S/\Delta S$  distributions for the  $B^0$  and non- $B^0$  samples. The long-lived  $B$  meson is seen to have a large  $S/\Delta S$ , so a cut at moderate  $S/\Delta S$  removes short-lived, two-

<sup>1</sup>In Figures 3, 4, 5, and 6, the number of entries represents the number of events that satisfied the cuts, including the underflow and overflow. When there are multiple histograms per plot, these summary numbers refer to only the unshaded data.

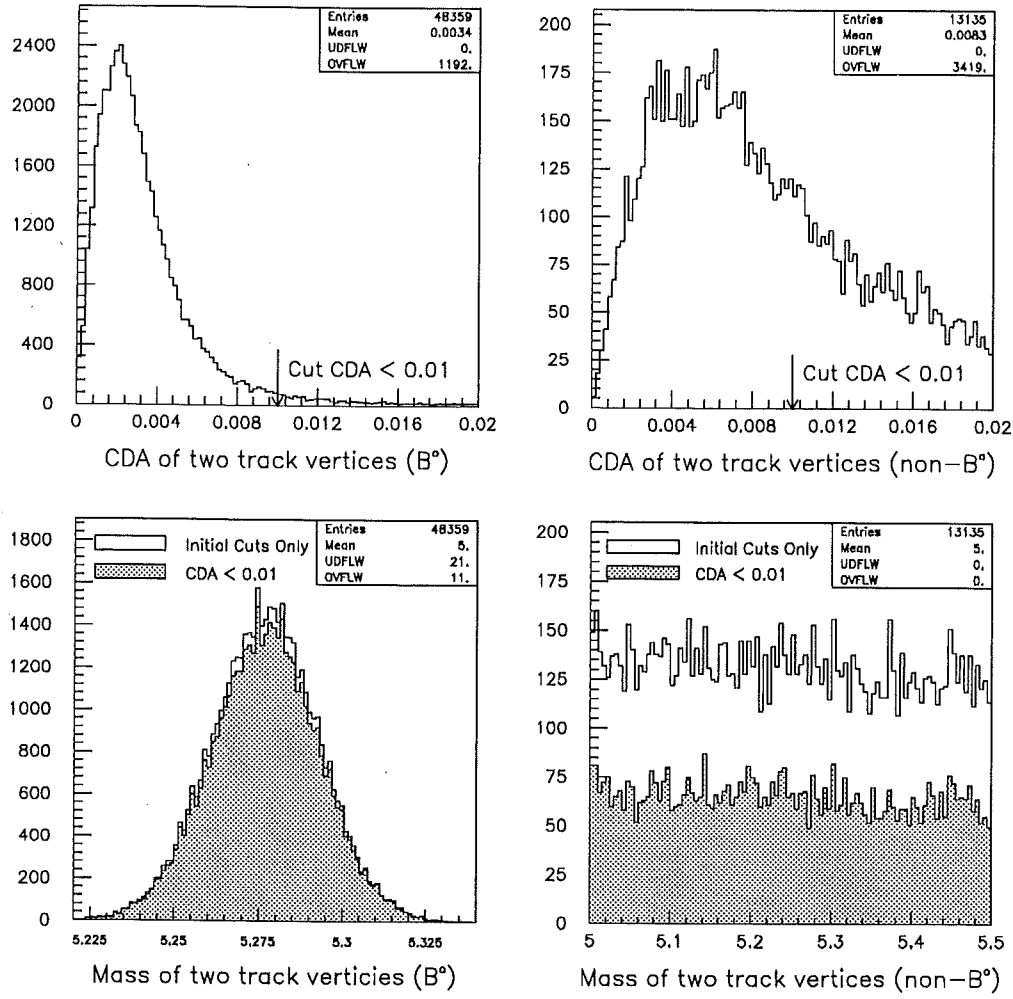


Figure 3: The effect of the CDA cut on  $B_d^0 \rightarrow \pi^+\pi^-$  decays from 1,040,000  $p$ - $p$  events at a center-of-mass energy of 40 TeV that each contained a  $b\bar{b}$  pair. All histograms show the data after the initial vertex  $\chi^2$ ,  $P_T$ , and  $|\eta|$  cuts.

track candidates from the non- $B^0$  sample. Events with  $S/\Delta S > 15$  were retained as  $B_d^0 \rightarrow \pi^+\pi^-$  candidates. The  $S/\Delta S$  cut eliminated 97% of the background and 52% of the signal. This suggests that most background  $B_d^0 \rightarrow \pi^+\pi^-$  decays contain tracks from the primary vertex that are poorly reconstructed.

Additional suppression of the non- $B$  background was obtained by requiring that both tracks of a candidate  $\pi^+\pi^-$  have transverse momenta above a specified value. Figure 5 shows the  $P_T$  distributions for a pion from  $B_d^0 \rightarrow \pi^+\pi^-$  decays, and also for pions of the non- $B$  candidate pairs. A cut at  $P_T = 1.75$  GeV/ $c$  on the first track of a non- $B$  pair eliminated 75% of such pairs, and 98% were eliminated when the cut was applied to both tracks. Meanwhile, the  $P_T$  cut 33% of the signal pairs.

The effect of combined cuts is shown in Figure 6. Note that none of the non- $B$   $\pi^+\pi^-$  candidates from nearly  $2 \times 10^6$  simulated events survived all three cuts.

Table 2 lists the cuts chosen and their effects on the signal-to-noise ratio for the decay  $B_d^0 \rightarrow \pi^+\pi^-$ . The first row shows the number of events remaining after the initial cuts on  $\chi^2$  of the primary and secondary vertices, and the initial  $P_T$  and pseudorapidity cuts on the pions. The following rows in the table show the effect of individual and combined cuts on the data. The signal-to-noise ratio was computed using the following expression:

$$S/N = \frac{S \times 10^{-5}}{\frac{4\sigma}{0.5} N}$$

where  $S$  is the number of signal events within  $\pm 2\sigma$  of the reconstructed mass of the  $B_d^0$  meson. For our assumption on the momentum resolution in the outer detector the  $B$ -mass resolution is 20 MeV/ $c^2$ .  $S$  was multiplied by  $10^{-5}$ , our estimate of the branching ratio for  $B_d^0 \rightarrow \pi^+\pi^-$ , because the decay  $B_d^0 \rightarrow \pi^+\pi^-$  was forced to have unit branching ratio in the GEANT simulation. The number of noise pairs over the  $4\sigma$  mass interval in which signal pairs were accepted was taken as the number  $N$  of noise pairs in the 0.5-GeV/ $c^2$  interval times  $4\sigma/0.5$  GeV/ $c^2$ . A flat noise distribution was assumed over the range of  $S$ . A confidence limit (CL) is stated for the last signal-to-noise ratio for the analysis with all cuts applied, as no background pairs survived. For data that follow a Poisson distribution, the 90% CL upper limit for the expected number of noise events when none are observed is 2.3 events. This number was used for  $N$  in the last row of Table 2 which shows the final signal-to-noise ratio at 90% CL.

We note that the signal-to-noise ratio scales inversely with the mass resolution, which may prove to be different in the actual experiment from that assumed here.

A simulation of 320,000  $p$ - $p$  interactions which produced light-quark pairs was made to investigate backgrounds in such events which constitute the bulk of the cross section at a hadron collider. Table 3 shows the reconstructed  $\pi^+\pi^-$  background in this and other data samples. The noise in the light-quark sample decreased faster than in the  $b\bar{b}$  sample as the cut strength increased. Although there will be 30-100 times as many light-quark events as those containing  $b\bar{b}$  pairs, the  $b\bar{b}$  events actually show a higher level of noise. It appears that the largest background of  $\pi^+\pi^-$  pairs



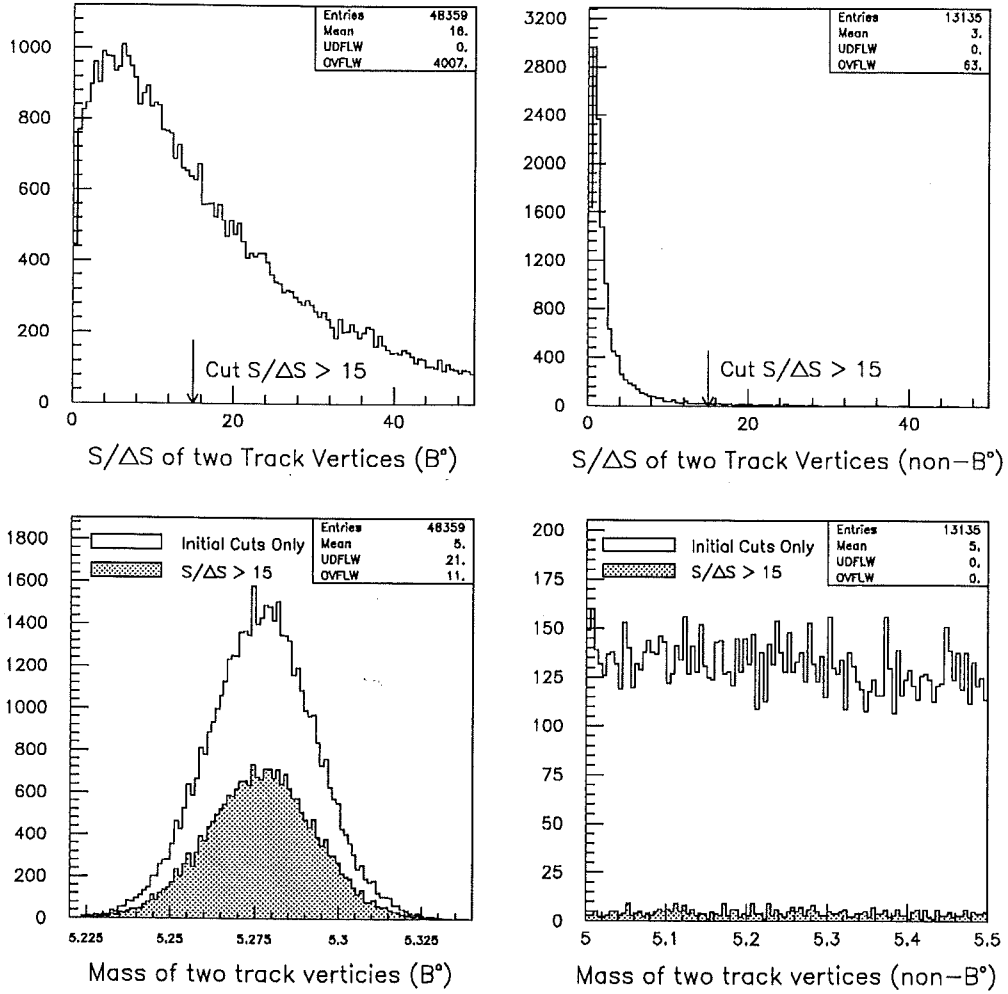


Figure 4: The effect of the  $S/\Delta S$  cut on  $B_d^0 \rightarrow \pi^+\pi^-$  decays from 1,040,000  $p$ - $p$  events at a center-of-mass energy of 40 TeV which contained  $b\bar{b}$  pairs. All histograms show the data after the initial vertex  $\chi^2$ ,  $P_T$ , and  $|\eta|$  cuts.

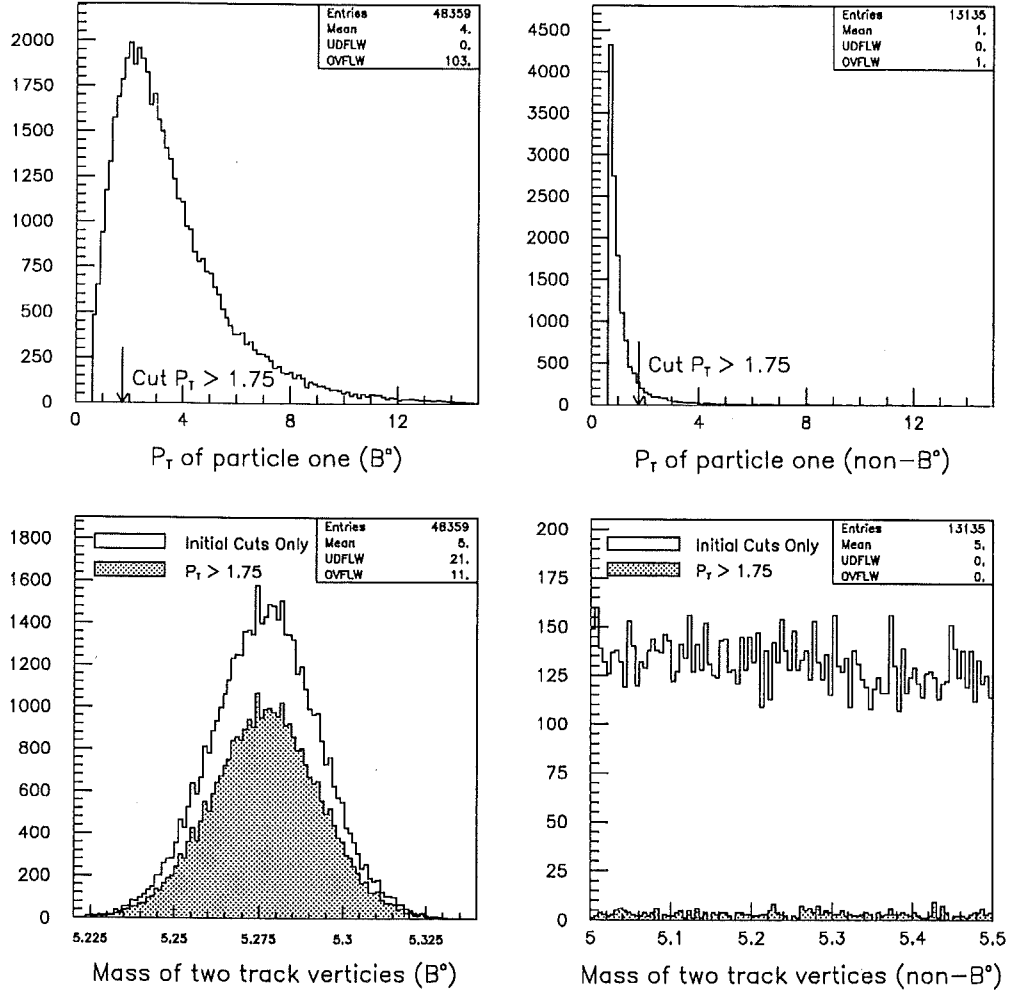


Figure 5: The effect of the  $P_T$  cut on  $B_d^0 \rightarrow \pi^+\pi^-$  decays from 1,040,000  $p$ - $p$  events at a center-of-mass energy of 40 TeV which contained  $b\bar{b}$  pairs. All histograms show the data after the initial vertex  $\chi^2$ ,  $P_T$ , and  $|\eta|$  cuts.

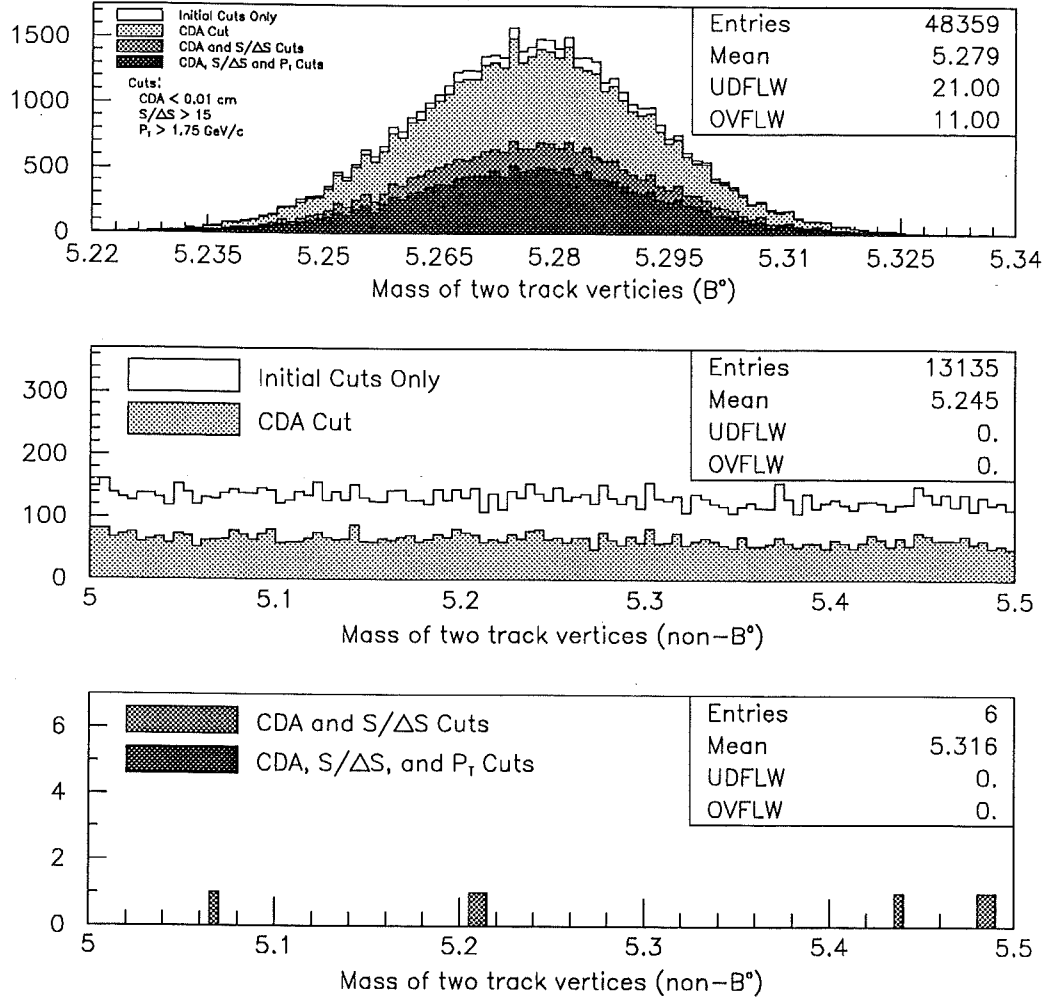


Figure 6: Top: the effect of all cuts on  $B_d^0 \rightarrow \pi^+\pi^-$  decays from 1,040,000  $p$ - $p$  events at a center-of-mass energy of 40 TeV which contained  $b\bar{b}$  pairs. Middle: the effect of the three initial cuts, and of the addition of the CDA cut on non- $B$   $\pi^+\pi^-$  pairs. Bottom: the effect of adding the  $S/\Delta S$  and  $P_T$  cuts on the non- $B$  pairs. No non- $B$  candidates survived the complete set of cuts within a  $0.5\text{-GeV}/c^2$  window around the  $B_d^0$  mass.

Table 2: Cuts and signal-to-noise ratios for  $B_d^0 \rightarrow \pi^+\pi^-$  decay candidates.

Cut	Cut Value	Signal $\times 10^{-5}$	Noise	Signal/Noise
Initial $\chi^2$ , $P_T$ and $ \eta $	3, 0.6 GeV/c and 4	46,023	13,135	0.00082
CDA	0.01 cm	43,532	6,508	0.00158
$S/\Delta S$	15.0	22,122	429	0.0123
$P_T$	1.75 GeV/c	30,980	321	0.0228
CDA and $S/\Delta S$	0.01 cm and 15	21,443	6	0.843
CDA, $S/\Delta S$ and $P_T$	0.01 cm, 15.0 and 1.75 GeV/c	15,527	0	$> 1.59$ 90% CL

not fitting to the primary vertex come from events in which one pion from a  $B$  decay combines with a poorly measured track from the primary vertex.

To determine whether charm decays might be misreconstructed as  $B$  decays we made a simulation of 400,000  $p$ - $p$  interactions containing  $c\bar{c}$  pairs. We were concerned that decays such as  $D^0 \rightarrow K^\pm\pi^\mp$  and  $D^0 \rightarrow \pi^+\pi^-$  could produce significant background contributions. However, as shown in Table 3, no events from this sample survived the cuts. We conclude that the contribution of charm quarks to the  $B_d^0 \rightarrow \pi^+\pi^-$  candidate sample to be less than the background from events containing  $b\bar{b}$  quarks.

Table 3: Cuts on the background to  $B_d^0 \rightarrow \pi^+\pi^-$  decays from  $p$ - $p$  collisions at a center-of-mass energy of 40 TeV for events containing various flavors of quarks.

Cut			Background Events Remaining		
Initial $\chi^2$ , $P_T$ and $ \eta $			13,135	2,478	2,389
CDA	$S/\Delta S$	$P_T$	$b\bar{b}$	light quark	$c\bar{c}$
0.150	3	0.75	1,638	67	111
0.100	5	0.75	831	38	47
0.050	10	1.00	86	2	4
0.025	12	1.50	14	0	0
0.010	15	1.75	0	0	0

## 5.1 $B^0 \rightarrow K\pi$ Analysis

A potential background in reconstructing the decay mode  $B_d^0 \rightarrow \pi^+\pi^-$  is  $B_d^0 \rightarrow K^+\pi^-$  where the  $K$  is assigned the  $\pi$  mass. A further background may arise from  $B_s^0 \rightarrow K^+\pi^-$  where the  $K$  is assigned the mass of the  $\pi$ . Unfortunately, the branching ratio of  $B^0 \rightarrow K\pi$  relative to  $B_d^0 \rightarrow \pi^+\pi^-$  is unknown and may approach unity. The calculation of these branching ratios are thought to be unreliable since it requires knowledge of penguin graphs. We have studied the overlap of the mass distributions of the above decay modes in the case where the  $K$  is assigned the mass of the  $\pi$ . We produced 120,000  $b\bar{b}$  where half of the  $B_d$ 's decayed into  $K^+\pi^-$  and the other half decayed into  $\pi^+\pi^-$  and all of the  $B_s$ 's decayed into  $K^+\pi^-$ . Figure 7 shows the overlap of the signal and noise distributions. We conclude that  $K$  identification will be necessary for any experiment wishing to measure  $B_d^0 \rightarrow \pi^+\pi^-$  since we observe significant overlap in the mass distributions.

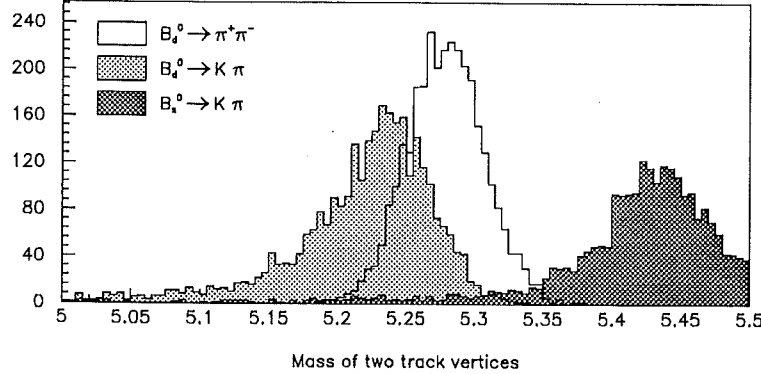


Figure 7: Mass distributions for  $B_d^0 \rightarrow \pi^+\pi^-$ ,  $B_d^0 \rightarrow K\pi$  and  $B_s^0 \rightarrow K\pi$  from  $p$ - $p$  interactions at a center-of-mass energy of 40 TeV. The  $K$  is misidentified as a  $\pi$ .

## 6 Conclusions

We have studied the feasibility of observing the decay mode  $B_d^0 \rightarrow \pi^+\pi^-$  in a hadron collider such as the SSC, using the ISAJET Monte Carlo and GEANT detector-simulation package. The large combinatoric background was the main concern. After cuts, principally on secondary-vertex quality, we achieved an efficiency for finding  $B_d^0 \rightarrow \pi^+\pi^-$  decays of 4% and a signal-to-noise ratio of  $> 0.42$ , 90% CL. The most serious background arises from incorrectly identified vertices in events containing  $b\bar{b}$

quarks. This simulation indicates that the SSC collider environment provides an opportunity to detect a large sample of  $B_d^0 \rightarrow \pi^+\pi^-$  events above background.

## Acknowledgments

We thank George Bourianoff of the SSC Laboratory for the use of the Accelerator Division 64-node iPSC/860 machine. We also thank Frank Paige for valuable discussions.

## References

- [1] E.L. Berger and R. Meng, *Heavy Quark Cross Sections at Hadron Collider Energies*, ANL-HEP-PR-92-11 (January 1992).
- [2] I.I. Bigi and A.I. Sanda, *CP Violation in Heavy Flavor Decays*, Nucl. Phys. **B281** (1987) 41.
- [3] F. Abe *et al.*, *Measurement of the B-Meson and b-Quark Cross Sections at  $\sqrt{s} = 1.8$  TeV Using the Exclusive Decay  $B^\pm \rightarrow J/\psi K^\pm$* , Phys. Rev. Lett. **68** (1992) 3403.
- [4] R.E. Hughes, *Reconstruction of B-Meson Decays and Measurement of the b-Quark and B-Meson Production Cross Sections at the Fermilab Tevatron Collider*, Ph.D. Thesis, University of Pennsylvania (1992).
- [5] A preliminary version of the present work has been reported in ref. [6] and more extensively in BCD Collaboration, *Response to the SSC PAC*, (July 11, 1990).
- [6] BCD Collaboration, *Bottom Collider Detector: A Low- and Intermediate- $P_t$  Detector for the SSC*, SSC-240 (Sept. 30, 1989); *Bottom Collider Detector, Expression of Interest* (EOI008), submitted to the SSCL (May 25, 1990).
- [7] P. Lebrun, *A Bottom collider Vertex Detector Design Monte Carlo Simulation and Analysis Package*, Fermilab TM-1682 (October 1, 1990).
- [8] L.A. Roberts, *Monte Carlo Simulation of Vertex Detector for Bottom Collider Detector*, Fermilab preprint FN-488 (June, 1988).
- [9] F.E. Paige and S.D. Protopopescu. *ISAJET 6.36*, Brookhaven National Laboratory.
- [10] R. Brun *et al.*, *GEANT3 User's Guide*, CERN DD/EE/84-1 (May 1986).
- [11] The particle database was based on J.D. Bjorken, *Estimates of Decay Branching Ratios for Hadrons Containing Charm and Bottom Quarks*, (1986, unpublished).

- [12] P.T. Keener *et al.*, *Porting of Standard High Energy Physics Physics Codes to the Intel iPSC*, submitted to Comp. Phys. Comm. (June 1992).
- [13] M. Lambrecht *et al.*, *Beam Tests of Silicon Microstrip Detectors with VLSI Readout*, IEEE Trans. Nucl. Sci. **NS-38** (1991).